A&A 501, 1103–1112 (2009)
DOI: 10.1051/0004-6361/200911823

Astronomy & Astrophysics

On the correlation between Ca and Hα solar emission and consequences for stellar activity observations

N. Meunier and X. Delfosse

Laboratoire d'Astrophysique de Grenoble, Observatoire de Grenoble, Université Joseph Fourier, CNRS, UMR 5571, 38041 Grenoble Cedex 09, France
e-mail: nadege.meunier@obs.ujf-grenoble.fr

Received 10 February 2009 / Accepted 22 April 2009

ABSTRACT

Context. The correlation between Ca and $H\alpha$ chromospheric emission, known to be positive in the solar case, has been found to vary between −1 and 1 for other stars.
Aims. Our objective is to understand the factors influencing this correlation in the solar case, and then to extrapolate our interpretation to other stars.
Methods. We characterize the correlation between both types of emission in the solar case for different time scales. Then we determine the filling factors due to plages and filaments, and reconstruct the Ca and Hα emission to test different physical conditions in terms of plage and filament contrasts.
Results. We have been able to precisely determine the correlation in the solar case as a function of the cycle phase. We interpret the results as reflecting the balance between the emission in plages and the absorption in filaments. We found that correlations close to zero or slightly negative can be obtained when considering the same spatio-temporal distribution of plages and filaments than on the sun but with greater contrast. However, with that assumption, correlations close to −1 cannot be obtained for example. Stars with a very low Hα contrast in plages and filaments well correlated with plages could produce a correlation close to −1.
Conclusions. This study opens new ways to study stellar activity, and provides a new diagnosis that will ultimately help to understand the magnetic configuration of stars other than the sun.

Key words. Sun: chromosphere – Sun: activity – Sun: filaments – Sun: magnetic fields – stars: activity – stars: chromospheres

1. Introduction

For the sun, the correlation between the emission in the Ca K and H lines and the emission in Hα is wellknown, as both follow the solar cycle (Livingston et al. 2007). However, this may not be the case for other stars, as shown by Cincunegui et al. (2007), who found that there was a large dispersion of such correlations. They have studied 109 stars, with a number of observations for each star ranging from a few to a maximum of 22 and covering about 7 years (total span of their observations). They found that for some stars, the correlation could be close to 0 and even negative. They do not provide any interpretation of this result.

There is therefore a need to understand the nature of this correlation. This type of observation can indeed be used as a diagnosis of stellar activity, but up to now no study has attempted to describe what kind of diagnosis could be derived. What can this correlation teach us about the nature of the stellar activity or the type of dynamo, for example?

To understand this, in this first paper (future work will be devoted to more accurate determination of this correlation for a large sample of stars), we study in detail this correlation in the case of the sun. We will first consider its dependence on cycle phase and the influence of the time span used to compute it. The Cincunegui et al. (2007) observations covered a range smaller than the solar cycle. When considering a short time span, we expect that a smaller correlation will be measured because of the small range of variation of the emission compared to the variability over short time scales. We use the measurements performed by Livingston et al. (2007) at Kitt Peak and covering 19 years to perform this study. This will allow us to determine if such a correlation varies over the solar cycle.

Then we attempt to understand this correlation by the contribution of emission in plages in Ca and Hα, which should lead to a correlation very close to 1, and of absorption in filaments, which should decrease the correlation because many of them are not associated directly with active regions and because their contrast is much lower in Ca than in Hα. We use Meudon spectroheliograms obtained between 1990 and 2002 in both Ca and Hα in order to estimate the relative contribution of plages and filaments in the solar case, and then to study their influence on the correlation between the two emissions. This provides clues to study the physics of stellar cycles, as it gives access to more information than the average activity level.

The outline of this paper is as follows. In Sect. 2, we study in detail the correlation between the Ca and Hα emission in the solar case, using Kitt Peak observations. In Sect. 3 we study Meudon spectroheliograms to estimate the contribution of plages and filaments to the observed correlation. These results are used in Sect. 4 to interpret the stellar observations of Cincunegui et al. (2007). We conclude in Sect. 5.

2. Analysis of Kitt Peak observations

In this section, we consider the sun as a star in order to study the correlation between the Ca and Hα emissions. For this purpose,

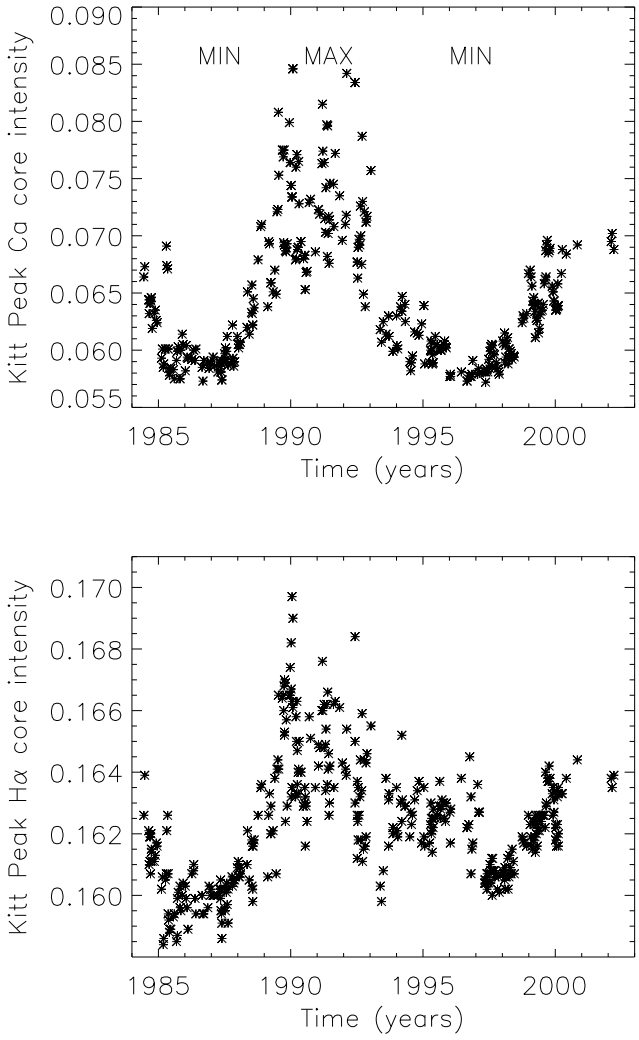

Fig. 1. *Upper panel*: emission in the Ca line versus time (from Livinsgton). *Lower panel*: emission in the Hα line versus time (from Livingston).

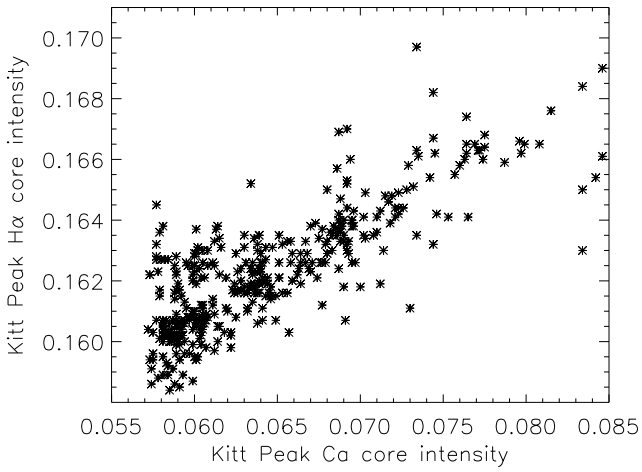

Fig. 2. Emission in the Hα line versus emission in the Ca line (from Livingston), from the 1984−2003 complete series. The correlation is 0.806 and the slope 0.27.

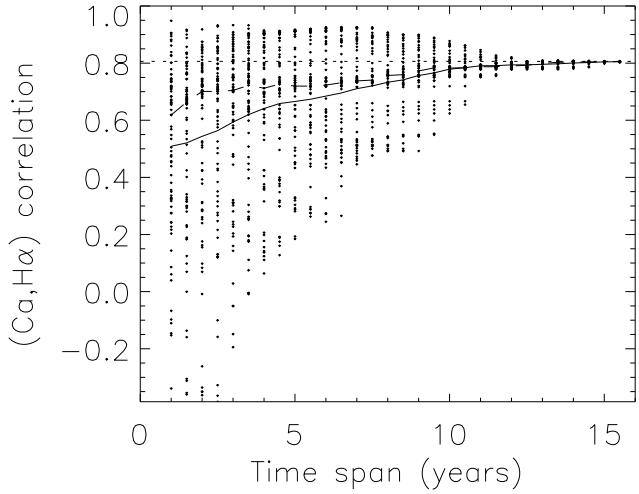

Fig. 3. Correlation between the emissions in the Ca and Hα lines, versus the time span. Each dot corresponds to a different cycle phase. The solid line represents the average and the dashed line the median. The horizontal dotted line corresponds to the correlation computed on the whole data set.

we use the long time series of observations performed at Kitt Peak by Livingston (Livingston et al. 2007)[1]. The sun was observed as a star (full-disk integrated light) using the Fourier Transform Spectrometer at Kitt Peak, thus providing spectra with a very high spectral resolution (about 500 000). The intensity in the line core of several lines is also available on the web[1].

2.1. Ca and Hα emission variations

We consider the intensity in the core for each of these lines, normalized by the continuum intensity (see Livingston et al. 2007, for more detail). Measurements cover the range 1984−2003 and consist of 383 observations. They therefore cover one and a half cycles, and are evenly spread over the full time range. Figure 1 shows the emission in both lines as a function of time. These variations are well correlated for example with the activity level defined by the spot number, as already known (Livingston et al. 2007): the correlation with the daily spot number is 0.86 for Ca and 0.78 for Hα.

[1] These data are available at
http://diglib.nso.edu/cycle_spectra.html

2.2. Correlation between the Ca and Hα emissions

We now study in more detail the relation between these emissions. We define the correlation factor between the two emissions E_{Ca} and $E_{\mathrm{H}\alpha}$ as:

$$C = \frac{\sum (E_{\mathrm{Ca}} - \overline{E_{\mathrm{Ca}}})(E_{\mathrm{H}\alpha} - \overline{E_{\mathrm{H}\alpha}})}{\sqrt{\sum (E_{\mathrm{Ca}} - \overline{E_{\mathrm{Ca}}})^2} \times \sqrt{\sum (E_{\mathrm{H}\alpha} - \overline{E_{\mathrm{H}\alpha}})^2}}.$$

We find a correlation of 0.806. The slope of the Ca emission versus the Hα emission is 0.27. This means that there is a strong correlation between the two, but it is different from 1. Departure from 1 could be due to noise in the data and/or to physical causes, which will be discussed later.

In Fig. 3, we study how the correlation varies with the phase of the solar cycle. We compute the correlation between the two emissions for different time lags and different starting times (i.e. different cycle phases) in the series. For each time span, all dots correspond to a different starting time in the series, covering the whole range (minus the time span). For short time spans,

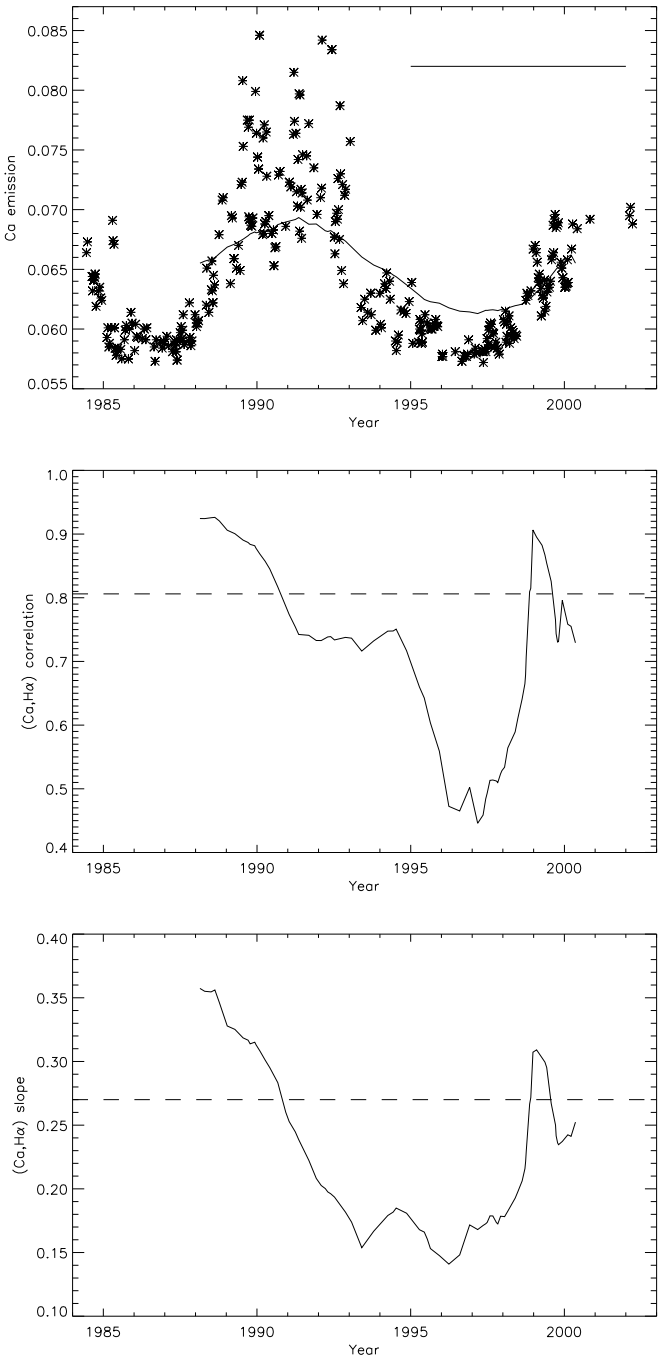

Fig. 4. *Upper panel*: original emission in the Ca line versus time (stars) and average over a time span of 7 years (solid line). The time corresponds to the middle of the 7 year span. *Middle panel*: correlation between the Ca and Hα emission versus time for a time span of 7 years. The horizontal dashed line corresponds to the full data set. *Lower panel*: Slope of the Hα emission versus the Ca emission for the same conditions.

very small correlations can be observed, including correlations close to zero or slightly smaller (∼−0.3), i.e. correlations are biased toward values smaller than the one obtained on long time scales. The correlation for our whole time serie is reached only for time spans close to the cycle length or larger.

Figure 4 shows the variation of the correlation over time, for a time span of 7 years (as used by Cincunegui et al. 2007). There is a strong relation between this correlation and the cycle phase. The correlation is indeed higher than average at the end of the ascending phase of the cycle (above 0.9) and much lower (about 0.45) at cycle minimum. Furthermore, the curve is not symmetric. For a given activity level, the correlation is higher during the ascending phase of the solar cycle compared to the descending phase. The behavior is similar for the slope.

3. Meudon spectroheliogram analysis

3.1. Contributions to the correlation between the Ca and Hα emission

We now explore possible causes for a correlation of less than 1 between the two emissions in the solar case. Active regions both show a strong emission in Ca and Hα due to plages and their position on the solar disk is similar, as shown in Fig. 5. However, the surface covered by the Hα plages is slightly smaller than the surface covered in Ca, as the latter are formed higher in the chromosphere. The chromospheric network is also more prominent in Ca than in Hα. We therefore expect a small dispersion between the two filling factors, that should lead to a correlation slightly lower than 1.

An important difference between the two is the presence of dark filaments at the surface, mostly visible in Hα. They are also slightly absorbing in Ca, but with a much lower contrast. When considering the integrated emission, their contribution will therefore be significant for Hα but not for Ca: they will decrease the correlation between the Ca and Hα emissions towards zero, because they do not coincide exactly with plages. On the other hand, if they were well correlated with plages, a strong filament contrast would lead to an anti-correlation. Filaments are cool and dense gas structures in the corona, maintained against gravity by the presence of a magnetic field. They are formed at the boundary between regions of opposite-polarity line-of-sight magnetic fields, either in the quiet sun or in active regions (see Martin 1998, for a review).

There are two different categories of filaments. Some are present in active regions, and these should naturally correlate well with the activity cycle both on short (days) and long time scales (cycle). However, they are usually small and very active, and therefore do not live very long. Therefore their contribution to the correlation should be small, as these properties are not compensated by very large numbers. Furthermore, those that are stable in active regions represent a small number, and they seem to show no correlation at all with the solar cycle (Mackay et al. 2008).

Secondly, there are also many large and stable quiescent filaments outside active regions. These filaments should therefore contribute significantly to the correlation. They seem to be correlated with the solar cycle (Mouradian & Soru-Escaut 1994; Li et al. 2007; Mackay et al. 2008), but again at a large scale (the cycle) and not necessarily at the scale of days or weeks. Even if their presence is related to active regions and in some way ultimately to large regions that are predominantly unipolar, the correlation may be low on small time scales, as there is a time delay between the active regions and the formation of these unipolar network regions.

3.2. Data analysis

To estimate the contribution of plages and filaments, we measure their filling factor over the solar cycle using Meudon spectroheliograms (provided by BASS2000[2]). As mentioned above, the

[2] http://bass2000.obspm.fr/home.php

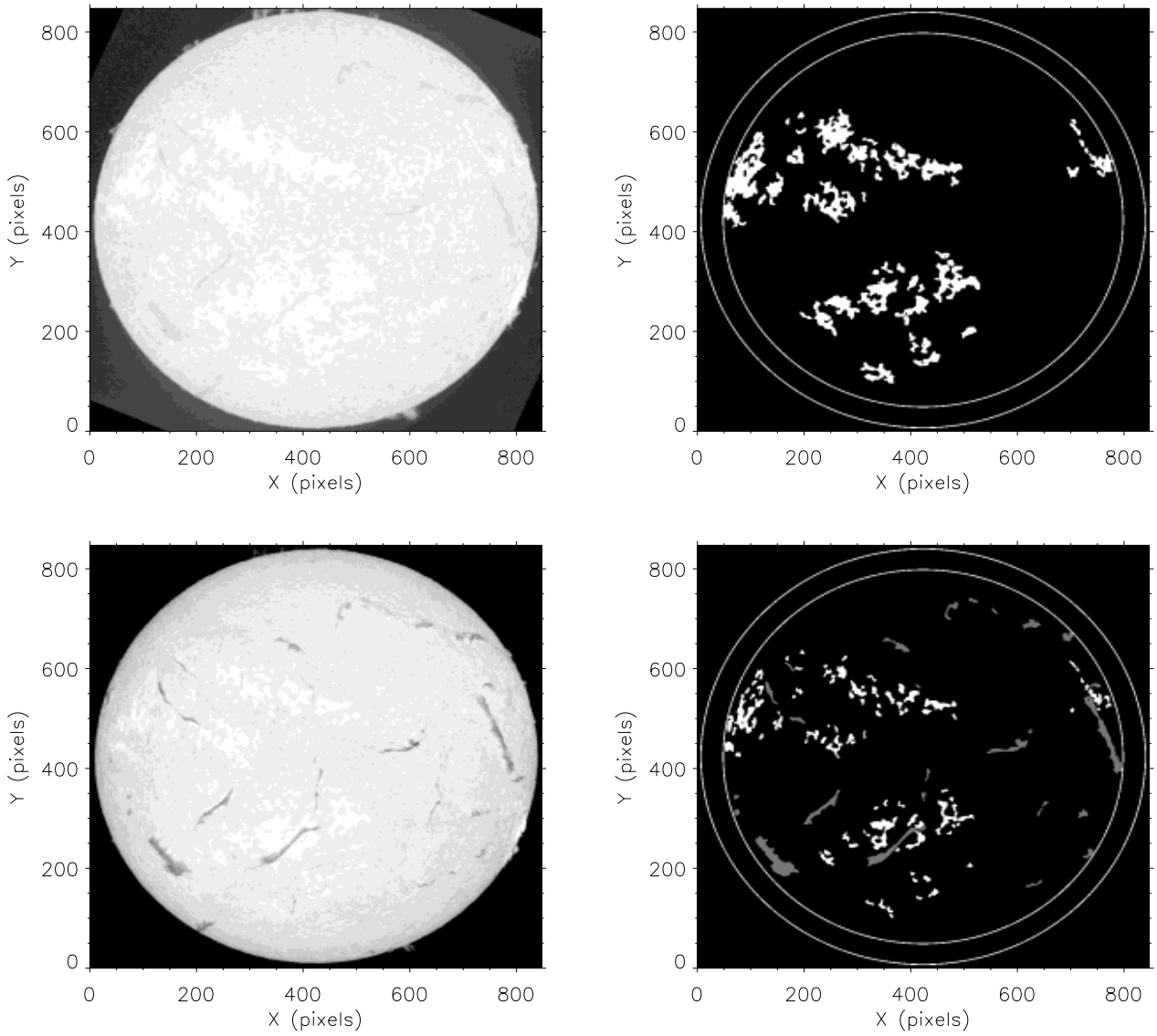

Fig. 5. *Upper panel*: a Ca spectroheliogram (*left*) and the corresponding segmented image (*right*). The outer ring shows the solar limb, and the inner ring the limit at $0.9 \times R_\odot$ used to select structures (plages in that case). *Lower panel*: same for Hα, with the bright structures corresponding to plages and the grey structures to filaments.

filament contrast in Ca is small, and we neglect it in the following. We therefore measure the plage filling factor both in Ca (taken at the center of the Ca II K line and showing the upper layer of the chromosphere) and in Hα images, and the filament filling factor in Hα images only. We have used numerized data obtained between 1990 and 2002, i.e. covering an 11-year solar cycle. Figure 6 shows the number of image pairs (Ca and Hα) for each 30 day period. There are 1690 pairs in our data set. There are naturally more images during the summer, due to the better weather. There are no large gaps in the data set, except for a few months in 1996, and the whole period is therefore well sampled.

It is beyond the scope of this paper to perform a very sophisticated region extraction such as those realized by Fuller et al. (2005), Ipson et al. (2005), Bernasconi et al. (2005), Aboudarham et al. (2008) or Scholl & Habbal (2008), as their purpose was to identify complete filaments as a whole, with Virtual Observatory applications in mind (building of synoptic maps for example, in which the different pieces constituting a filament must be associated and tracked in time). Here we are mainly interested in the total area covered by these structures at a given time, therefore there is no need to associate them. This considerably simplifies the segmentation step. For the same reason, we do not attempt to use all data, and have therefore selected the best images (reasonable seeing, no clouds, no large dust line). Therefore our algorithm, although presenting strong similarities with these previous works, is more simple. It is constituted of the following steps: center-to-limb darkening correction; analysis of the intensity histograms in order to determine a threshold (ensuring robustness of the final filling factor over time); application of this threshold to the data; application of a thinning procedure; analysis of the segmented data to extract the size of the structures. Structures smaller than 10 pixels are eliminated (see further for more discussion on the size threshold).

A size selection is performed to eliminate the smallest structures, as we focus on plages and active network to reduce the noise. This size threshold is applied only to the Ca structures (and fixed at 120 Mm^2). We have tested thresholds between 30 Mm^2 (corresponding to about 10 pixels and therefore very noisy) and 270 Mm^2 (corresponding to small active regions). The chosen threshold corresponds to the smallest structures that

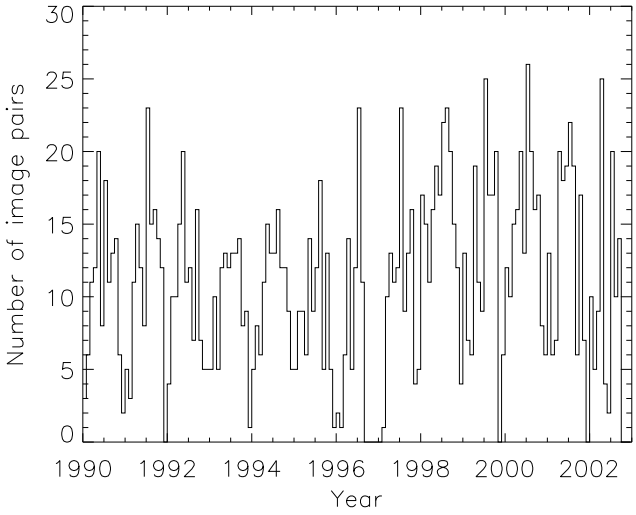

Fig. 6. Number of image pairs in the Meudon data set.

did not significantly influence the results and allows us to take into account a significant proportion of the magnetic network. As the very small structures have a lower contrast (Worden et al. 1998), it is not a problem to eliminate them at this stage. Then we only keep structures that are overlapping in both wavelengths. This step makes the procedure robust by eliminating small features that would appear in one of them only due to the threshold choice, if their size were to be close to the threshold. For the same reason, we have selected filaments with the same threshold (sizes larger than 120 Mm^2), but the influence is not significant either because the smallest features do have a very low contrast as well and therefore do not influence the integrated emission. As shown in Fig. 5, large filaments are well defined, however we do miss the thinnest filaments, which are present mostly in active regions. Because these are much thinner and short-lived, they are the filaments which contribute the less, so it is not a critical point (see Sect. 3.1 for a discussion).

Finally, a filling factor is computed using the selected structures (surface divided by the total surface of the sun on the image). We are mostly interested in the variability of these filling factors and the correlation between them, more than in the absolute values of the filling factors themselves, so the exact thresholds used to extract the structures is not as sensitive as it would be to get the exact size of these structures for example.

3.3. Filling factors over the cycle for active regions and filaments

Figure 7 shows the resulting filling factor versus time for the 3 types of structures: plages identified on Ca II K images (ff_{Ca}), plages identified on Hα images ($ff_{\mathrm{H}\alpha}$), and filaments identified on Hα images as well (ff_{fil}). As expected, we observe a strong correlation of 0.92 between the plage filling factor in Ca images and in Hα images. The filament filling factor is also higher at cycle maximum, but the correlation with the plage filling factor is lower, with values of 0.52 for Ca and 0.53 for Hα.

Figure 8 also shows $ff_{\mathrm{H}\alpha}$ and ff_{fil} versus ff_{Ca}. The correlation is quite clear in both cases. For Hα plages, the relation is close to linear with a change in slope for ff_{Ca} around 0.04: at higher activity levels, $ff_{\mathrm{H}\alpha}$ increases faster than ff_{Ca}. This may be due to the largest structures at that time, with therefore a ratio closer to one between the size of the regions observed in Ca and Hα. As for filaments, a linear increase is observed for ff_{Ca} up to 0.06,

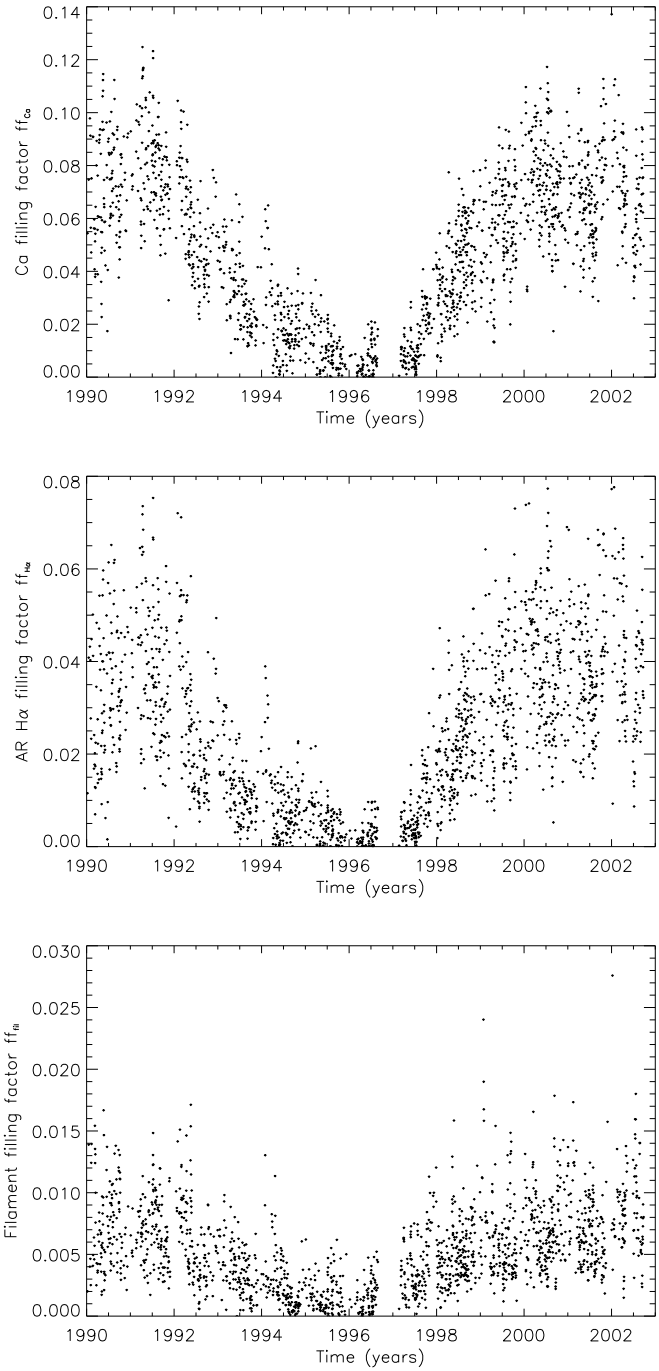

Fig. 7. *Upper panel*: filling factor of Ca II K plages. *Middle panel*: filling factor of Hα plages. *Lower panel*: filling factor of filaments.

and then a saturation (corresponding to cycle maximum): above a certain activity level, the filament filling factor remains constant, which is a new result. This and the large dispersion explain the correlation close to 0.5, i.e. far from 1. We also note that at cycle minimum, when ff_{Ca} and $ff_{\mathrm{H}\alpha}$ both go very close to zero, ff_{fil} is significantly above zero, showing the presence of a significant number of filaments, as already observed (Makarov & Mikhailutsa 1992; Mouradian & Soru-Escaut 1994).

The different time scales will be important when interpreting stellar data. On a long time scale (cycle period for example), the filament filling factor is roughly correlated with the activity level (determined from the Ca filling factor for example), as already pointed out by Mackay et al. (2008) for a few selected

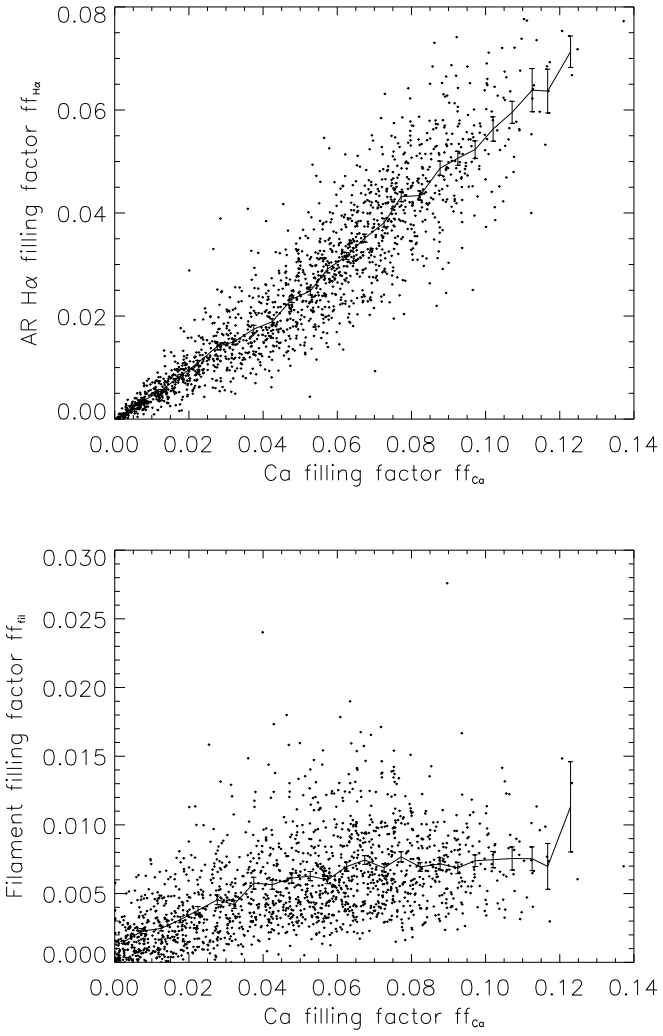

Fig. 8. *Upper panel*: filling factor of Hα plages versus filling factor of Ca II K plages. *Lower panel*: filling factor of filaments versus filling factor of Ca II K plages.

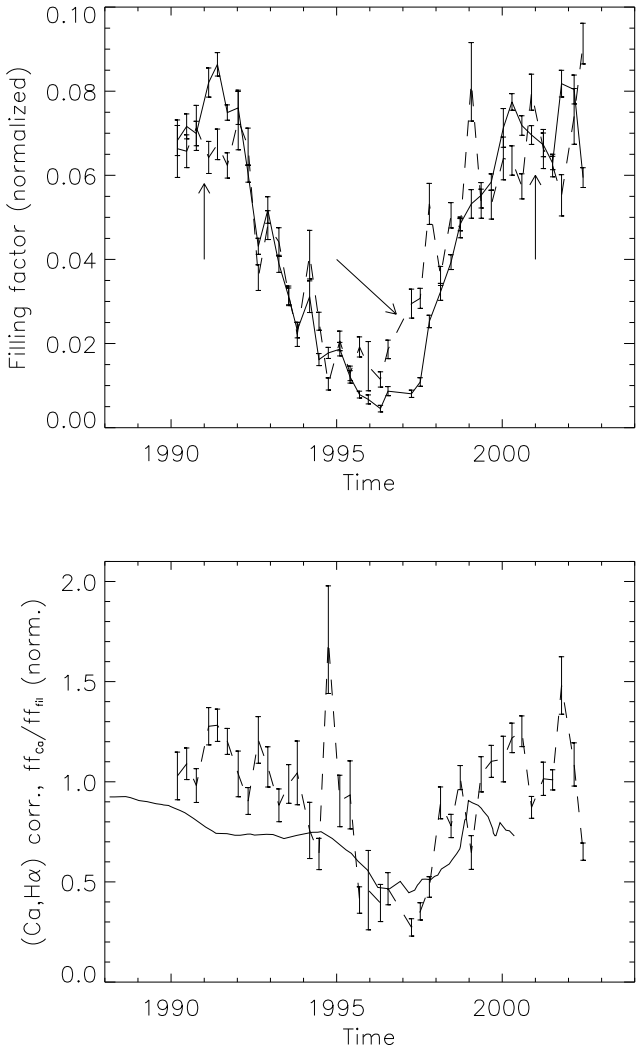

Fig. 9. *Upper panel*: Ca filling factor ff_{Ca} (solid line) and filament filling factor ff_{fil} normalized to the same median (dashed line), both averaged of 4 rotation periods, versus time. *Lower panel*: correlation between the Ca and Hα Kitt Peak emission versus time (solid line, from Fig. 4, *middle panel*) superimposed on the ratio (dashed line) between the two upper curve ($ff_{\mathrm{Ca}}/ff_{\mathrm{fil}}$ with a normalization of ff_{fil} as in *the upper panel*).

periods over the cycle. In addition to the saturation at high activity levels found above, the correlation is not close to 1 due to a large dispersion, and this means that at small time scales (rotation period) the correlation could be much closer to zero. Finally, Fig. 9 shows the filling factors for Ca and filaments for an averaging over temporal windows of about 4 rotation periods. On this plot, ff_{fil} has been normalized to ff_{Ca} (same median) to make the comparison easier. The correlation at this large temporal scale is now much closer to 1 (0.87) due to the temporal smoothing. The value of 0.92 (as for ff_{Ca} and $ff_{\mathrm{H}\alpha}$ obtained above) is found for a temporal smoothing of about 200 days. There are, however, a few noticeable differences. At cycle minimum and during the beginning of the ascending phase, the surface covered by filaments increases faster than the plage filling factor. On the other hand, at cycle maximum, the peaks are not as sharp, especially for the 1990–1991 maximum, which is related to the saturation above. The cycle maximum in 2000–2002 is known to exhibit two peaks, as shown by the ff_{Ca}: this is not observed for filaments, with in fact a peak in between, shifted by about 200–300 days from the first peak. Figure 9 also shows that the dip in the ratio between the plage and filament filling factors observed around 1996–1997 corresponds to the low correlation factor observed in the Kitt Peak emission at that time, which reinforces our interpretation of the correlation evolution by the presence of filaments.

3.4. Reconstruction of the emission

In using contrasts for plages in Ca and Hα, and for filaments in Hα (C_{Ca}, $C_{\mathrm{H}\alpha}$ and C_{fil} respectively), it is possible to reconstruct the emissions in Ca and Hα as defined by:

$$E_{\mathrm{Ca}} = C_{\mathrm{Ca}} \times ff_{\mathrm{Ca}}$$
$$E_{\mathrm{H}\alpha} = C_{\mathrm{H}\alpha} \times ff_{\mathrm{H}\alpha} - C_{\mathrm{fil}} \times ff_{\mathrm{fil}}.$$

In the following, we have assumed constant contrast over time. We have also considered the same contrast for structures of all size. We know that for bright structures, there is a variability depending on their size from plages down to the network (Worden et al. 1998), however in this work we focus mostly on plages (see Fig. 5), so we do not expect a large effect.

Unfortunately, the available Meudon data alone do not allow us to compute the plage and filament contrast, as there is no intensity calibration. It is, however, possible to determine them

Table 1. Correlations and parameters from a fit in the Kitt Peak data or from the literature.

Type	Variable	Kitt Peak	Fit	Literature
Obs.	Corr($ff_{\rm Ca}$, $ff_{\rm H\alpha}$)	...	0.923	0.923
	Corr($ff_{\rm Ca}$, $ff_{\rm fil}$)	...	0.524	0.524
	Corr($ff_{\rm H\alpha}$, $ff_{\rm fil}$)	...	0.520	0.520
Param.	$C_{\rm Ca}$	...	0.20	0.70
	$C_{\rm H\alpha}$	...	0.13	0.35
	$C_{\rm fil}$	...	0.30	0.20
Constr.	Corr($E_{\rm Ca}$, $E_{\rm H\alpha}$)	0.805	0.805	0.913
	Slope($E_{\rm Ca}$, $E_{\rm H\alpha}$)	0.267	0.268	0.260
	Ampl. $E_{\rm Ca}$	0.028	0.028	0.096
	Ampl. $E_{\rm H\alpha}$	0.012	0.013	0.027
	χ^2	...	0.0009	0.109

Note1. The first 3 lines provide the correlation between the observed filling factors. The following set of lines gives the contrasts which have been used (either from a fit on from the literature). The last set of lines shows the constrains that can be used to either constrain the fit or, in the last column, to test the contrasts found in the literature, compared to the values expected from the Kitt Peak observations.

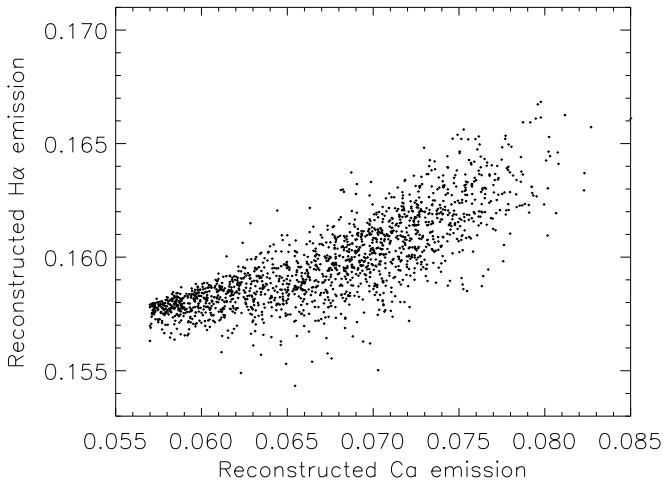

Fig. 10. Reconstructed emission in Ca II K versus the reconstructed emission in Hα.

using both Meudon and Kitt Peak data. We have estimated the best contrasts $C_{\rm Ca}$, $C_{\rm H\alpha}$ and $C_{\rm fil}$ that would lead to reconstructed emissions varying over a range similar to that observed at Kitt Peak. We also constrain these contrasts by adjusting them in order to obtain a correlation and a slope between the reconstructed emissions as close as possible to the Kitt Peak values. We therefore minimize a χ^2 which takes into account these three factors, equally weighted. The smallest χ^2 then provides the best estimates for the three contrasts. Using these contrasts and the observed filling factors, we derive the reconstructed emissions $E_{\rm Ca}$ and $E_{\rm H\alpha}$. We find contrasts that reproduce the Kitt Peak observations (see Table 1). These contrasts correspond to a small band pass, as we are using Kitt Peak intensities in the line core. Figure 10 shows $E_{\rm H\alpha}$ versus $E_{\rm Ca}$ in that case and can be compared to the Kitt Peak observations in Fig. 2. We note that despite the same amplitude, correlation and slope, the behavior is slightly different, as Kitt Peak observations exhibit the largest dispersion for small activity levels, while here the largest dispersion is for large activity levels.

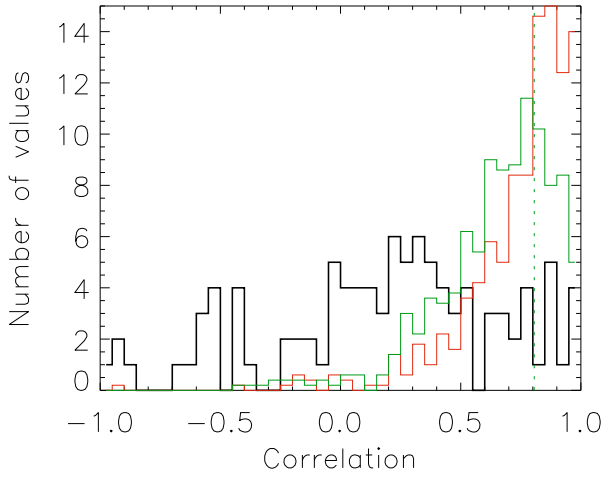

Fig. 11. Comparison of the distribution of correlations obtained by Cincunegui et al. (2007) for a sample of 109 stars (solid line) and for the sun viewed from the equator normalized to the same number of stars (this work) for various phase of the solar cycle and a similar time span, i.e. 7 years (red line). The green line is derived from the same conditions as for the red line, but takes into account a uniform distribution of inclination angles between 0 and 90° for a latitudinal extent of [−30°, 30°] for plages and [−60°, 60°] for filaments (see Sect. 4.1 for details).

Another possibility is to use the contrasts published in the literature. Unfortunately, we did not find any large and systematic studies that would provide all necessary contrasts. One reason is that they depend significantly on the band pass and that there are few studies on a large sample. For Ca structures, we have used the value of 0.7 deduced from Worden et al. (1998), who obtained a variation with the type of structure (from the network to plages). Ortiz & Rast (2005) also observed a variation of the Ca contrast as a function of the line-of-sight magnetic field. We considered the value of 0.35 for $C_{\rm H\alpha}$, assuming a factor of two between Ca and Hα (Kononovich & Nikulin 1975). This ratio of 2 is close to what we obtained above with the fit. The filament contrasts show a very large dispersion in the literature and we have taken an average value of 0.2 deduced from Maltby (1976) and Chae et al. (2006). As shown in Table 1, the χ^2 is much worse in that case, and it is not possible to reproduce the observed amplitude of variation and the correlation, as the plage contrasts are too high and the filament contrast too low. This may be due to the difference between the band pass at which they were measured (0.5 Å for example in the case of Worden et al. 1998) and the Kitt Peak observations we are using.

4. Toward diagnosis of stellar activity

4.1. Distribution of stellar and solar correlations

Figure 11 shows the distribution of correlations obtained by Cincunegui et al. (2007). They observe a significant number of stars with correlations close to zero or negative. Superimposed on it, we show the distribution in the case of the sun, for a time span of 7 years (red line), and covering different phases of the solar cycle, deduced from the dots of Fig. 3 for that time span. Several conclusions can be drawn from this comparison.

First, the two distributions are very different, as the tail toward small correlations is of small amplitude in the case of the sun, compared to the number of cases around 0.8. However, Cincunegui et al. (2007) provide no uncertainties on the

correlations, and some of these are large (given the available plots). However, large uncertainties probably do not suffice to explain the difference in distribution. This means that the activity of the sun is probably not typical of that of other stars, possibly due to filaments. A possible source of discrepancy could be the heterogeneity in the sample studied by Cincunegui et al. (2007) in terms of stellar type.

It is also necessary to take into account the large range of inclination angles present in stellar observations. In the solar case, the latitudinal extent of plages and filaments is different, so one can expect a different contribution from these two types of structures depending on the inclination angle. If considering that plages extend up to 30° and filaments up to 60°, for example, and assuming that the filling factor at each time step is attributed to that latitudinal range, a correlation of 0.8 (sun viewed from the equator) would fall to 0.75 for an inclination angle of 45° and to 0.49 for a pole-on orientation. For a uniform distribution of inclination angles between 0 and 90°, the distribution shown in Fig. 11 (red line) should then be smeared toward lower correlations and is shown in green.

The second conclusion is that despite these differences, the solar distribution exhibits small correlations in a few cases. This means that if stellar observations do not cover a full activity cycle (or more generally, the full range of activity existing for that star), we are likely to significantly underestimate the correlation with respect to the one that would be obtained when considering a full cycle. In that case, the only way to consider the data is a statistical analysis of a large number of stars, i.e. via the distribution of correlations. Indeed, for a given star, the correlation may be low (for example close to zero) even if in reality the star has a correlation computed over the whole cycle similar to the solar one. If the cycle length is known, as well as the phase, it may be possible, in principle, to apply a correction deduced from the plot of Fig. 4 (or a similar one if the time span of the observations is different). In that case, a distribution of corrected correlations could be produced, that would give an indication of the true correlations over the whole activity range. However, such corrections would assume a behavior similar to the sun (in particular, relative contrast).

4.2. Influence of the filament contrast on the correlation

We now consider cases for which the correlation is computed over the whole cycle. It would also be interesting to know what the sensitivity is of the correlation for filament contrasts differing from the solar contrasts found above. Figure 12 shows the correlation between the reconstructed emission in Ca and Hα for various filament contrasts, while keeping the same contrasts for plages in Ca and Hα. For low contrast, the correlation is naturally close to 1. For increasing filament contrast, the correlation decreases, crosses zero for a certain contrast, and then saturates for values around −0.4. Table 2 shows the contrast necessary to reach a correlation of zero as well as the ratio to the solar contrast. A contrast 3.9 times the solar value of 0.30 (i.e. 1.16) and the same distribution in time and position of the filaments would lead to a correlation close to 0. The factor is, of course, the same when applied to the area covered by the filaments instead of their contrast. When using the contrast obtained from the literature, the filament contrast necessary to reach a zero correlation is much higher. A contrast of 1.16 is larger than 1, which means that a correlation of zero for the same spatio-temporal organization of the filaments can be reached only if the filling factor of filaments is increased. We see that, for example, for a factor 2 increase in contrast and in size, which is not very extreme (the observed contrast of individual solar filaments varies by a factor of 3−4), at least such a zero correlation is reached.

However, we cannot obtain a strong negative correlation below ∼−0.4, and such values correspond to extreme conditions compared to the sun. Therefore, the spatio-temporal organization of filaments must be significantly different if the presence of filaments explains the Ca − Hα relation observed in other stars. For example, filaments that would be more strongly in phase

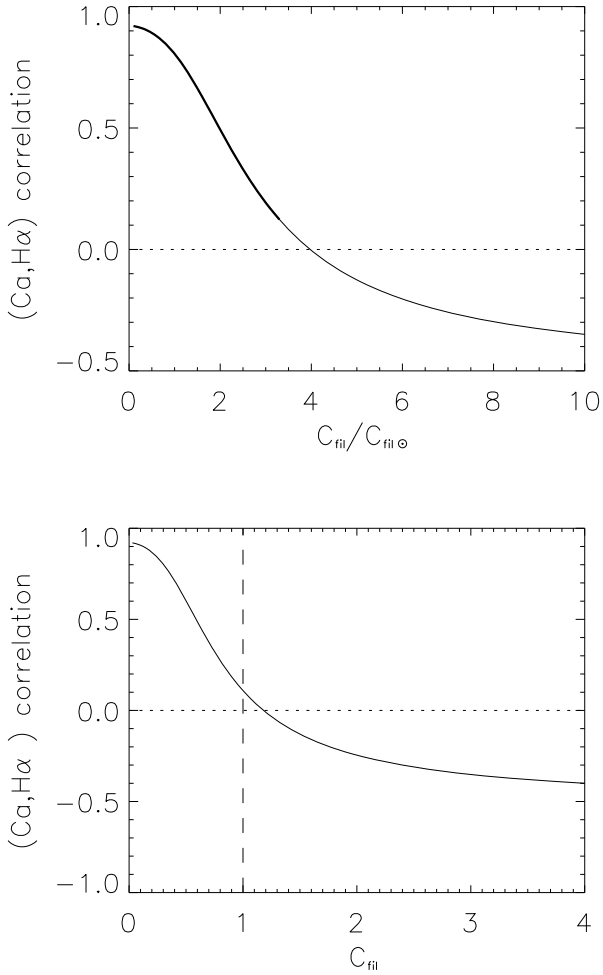

Fig. 12. *Upper panel*: correlation between the reconstructed emission in Ca II K and Hα for various filament contrasts (relative to the fitted solar value). *Lower panel*: same versus the actual filament contrast, without the normalization to the solar value.

Table 2. Filament contrasts for which the correlation is equal to zero.

Contrast	Fit	Literature
$C_{\rm Ca}$	0.20	0.70
$C_{\rm H\alpha}$	0.13	0.35
$C_{\rm fil}$	0.30	0.20
$C_{\rm fil}$(corr = 0)	1.16	3.08
$C_{\rm fil}$(corr = 0)/$C_{\rm fil}$	3.9	15.4

Note 2. Given the fitted contrasts for the three types of structures or those found in the literature, a filament contrast for which the correlation is equal to zero is given, in absolute value and relative to the solar value (see Sect. 4 for details).

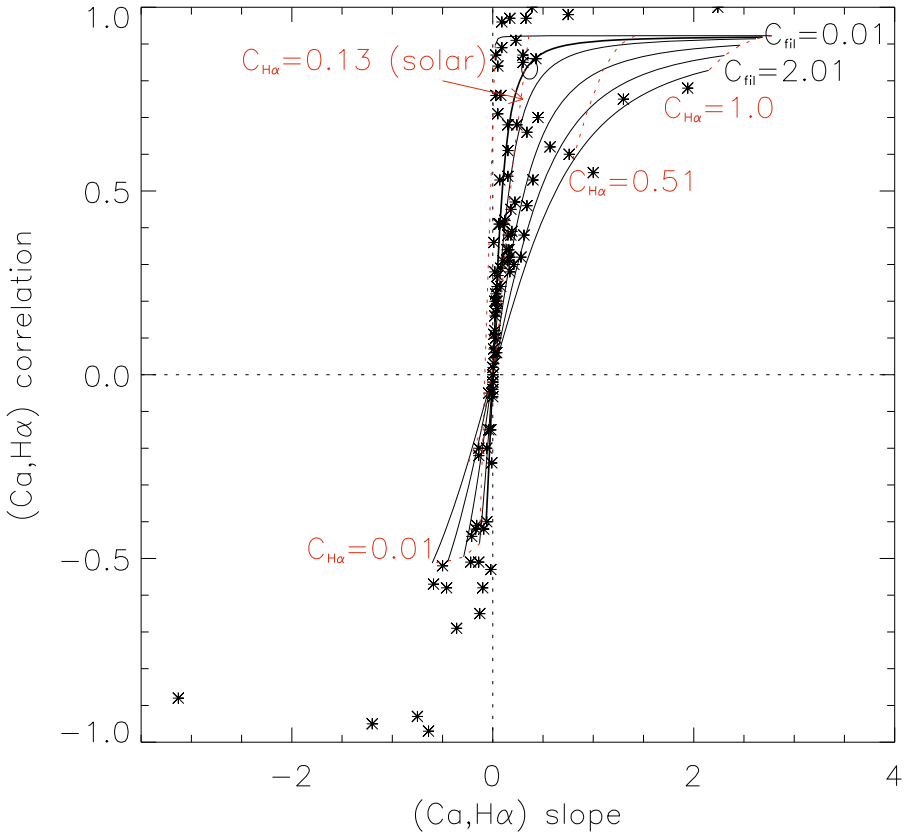

Fig. 13. Correlation between the Ca and Hα emission versus the slope, for the Cincunegui et al. (2007) results (stars) and the sun (circle). A model corresponding to the solar $C_{\rm fil}$ and a variable $C_{\rm H\alpha}$ is superimposed (thick line), as well as 5 models (thin lines), each of them with a different $C_{\rm fil}$ (from a low filament contrast for the upper curve to a high filament contrast for the lower curve). For each curve, $C_{\rm H\alpha}$ varies from 0.01 to 1. $C_{\rm Ca}$ is constant (fitted solar value of 0.20).

with plages and with a contrast dominating that of Hα plages could lead to an anti-correlation.

4.3. *Influence of the filament and plage contrasts on the correlation*

We now look at the influence of all contrasts on the correlation and the slope simultaneously. Figure 13 shows the correlation versus the slopes as observed by Cincunegui et al. (2007) superimposed with the expected correlations and slopes for solar filling factors multiplied by various values of the Hα plage contrast (between 0 and 1) and of the filament (between 0 and 2, i.e. allowing a larger filling factor for the filaments). Most stars could then be explained by this interpretation, i.e. with the assumption that plages and filaments have the same spatio-temporal distribution than on the sun but different contrasts. The most notable exceptions are a few stars with correlations very close to −1. There are also a few stars with correlation between 0.92 (the solar case with no filament) and 1 but the uncertainties on the correlation in these stellar observations are larger than this difference.

This graph showing the correlation versus the slope allows us to explore different physical conditions that may be found on stars of different types (e.g. different temperature and density profiles in the chromosphere). The value of the correlation depends significantly on several factors. First, it depends on the ratio between the plage contrast and the filament contrast, as shown in Sect. 4.2. It also varies with the ratio between the plage contrast in Ca and Hα. These lines are not formed at the same level in the chromosphere, and we could expect stars of different types to exhibit a ratio different from the solar value. For stars with a Hα contrast much smaller than the Ca one, the correlation falls rapidly to zero or to negative values.

5. Conclusion

The first result of this work is a precise characterization of the correlation between the Ca and Hα emission in the solar case: the value of the correlation, dependence on the time scale and cycle phase, and finally interpretation using filaments, which decrease the correlation due to plages. Also, we have found that the filament filling factor is correlated to the activity level (0.5) but with a large dispersion (due to the low correlation at short time scales) and a saturation effect at high activity levels, which is new.

In addition, we can use these results to estimate what would be expected on stars with a similar spatio-temporal distribution of filaments and plages but different sizes or contrasts. We can explain most of the results obtained by Cincunegui et al. (2007), but not all of them. This may reflect physical conditions different from solar, either in chromospheric properties or in the activity cycle. However, the uncertainties in the results obtained by Cincunegui et al. (2007) seem to be quite large and they could be responsible for the observed discrepancy with the solar case. There is therefore a need to study in more detail the precise relationship between the Ca and Hα emissions in a large star sample. This is probably at least partially due to the poor temporal sampling. This is also necessary because their sample is quite heterogeneous in stellar types. This is a work in progress.

If we want to extrapolate to stellar cases with different magnetic configurations and consequently a different spatio-temporal distribution of filaments, we need to obtain a better estimate of the filament behavior over the solar cycle. We therefore plan to study this using the very large data set of MDI/SOHO magnetograms (Scherrer et al. 1995). This will allow us to establish a link to the magnetic configuration.

Acknowledgements. The Kitt Peak observations kindly have been made available on the web by W. Livingston. We thank W. Livingston and R. Toussaint for their comments on these data. The Meudon spectroheliograms were provided by BASS2000. We thank J. Aboudarham for informations on these data. The monthly sunspot number was provided by the SIDC-team, World Data Center for the Sunspot Index, Royal Observatory of Belgium, Monthly Report on the International Sunspot Number, online catalogue of the sunspot index: http://www.sidc.be/sunspot-data/, 1984−2003. We thank the anonymous referee for his/her comments.

References

Aboudarham, J., Scholl, I., Fuller, N., et al. 2008, Annales Geophysicae, 26, 243
Bernasconi, P. N., Rust, D. M., & Hakim, D. 2005, Sol. Phys., 228, 97
Chae, J., Park, Y.-D., & Park, H.-M. 2006, Sol. Phys., 234, 115
Cincunegui, C., Díaz, R. F., & Mauas, P. J. D. 2007, A&A, 469, 309
Fuller, N., Aboudarham, J., & Bentley, R. D. 2005, Sol. Phys., 227, 61
Ipson, S. S., Zharkova, V. V., Zharkov, S., et al. 2005, Sol. Phys., 228, 399
Kononovich, E. V., & Nikulin, I. F. 1975, SvA, 18, 602
Li, K. J., Mu, J., & Li, Q. X. 2007, MNRAS, 376, L39
Livingston, W., Wallace, L., White, O. R., & Giampapa, M. S. 2007, ApJ, 657, 1137
Mackay, D. H., Gaizauskas, V., & Yeates, A. R. 2008, Sol. Phys., 248, 51
Makarov, V. I., & Mikhailutsa, V. P. 1992, Sol. Phys., 137, 385
Maltby, P. 1976, Sol. Phys., 46, 149
Martin, S. F. 1998, Sol. Phys., 182, 107
Mouradian, Z., & Soru-Escaut, I. 1994, A&A, 290, 279
Ortiz, A., & Rast, M. 2005, Mem. Soc. Astron. Ital., 76, 1018
Scherrer, P. H., Bogart, R. S., Bush, R. I., et al. 1995, Sol. Phys., 162, 129
Scholl, I. F., & Habbal, S. R. 2008, Sol. Phys., 248, 425
Worden, J. R., White, O. R., & Woods, T. N. 1998, ApJ, 496, 998